*Fibers and Polymers* 2021, Vol.22, No.9, 2588-2601
DOI 10.1007/s12221-021-0164-1

ISSN 1229-9197 (print version)
ISSN 1875-0052 (electronic version)

# Dielectric Properties of Composites of Natural Rubber and Keratin Fibre from Chicken Feather

**Divia P. Sreenivasan[1], Sujith A[2], Avinash Nelson Asokan[3], and Rajesh C[1]***

[1]*Department of Chemistry, MES Keveeyam College, Valanchery-676552, Kerala, India*
[2]*Department of Chemistry, National Institute of Technology, Calicut-673601, Kerala, India*
[3]*Department of Electrical and Electronics Engineering, Government Engineering College, Wayanad-670644, Kerala, India*

(Received October 2, 2020; Revised December 25, 2020; Accepted January 6, 2021)

**Abstract:** The dielectric properties of chicken feather fibre-natural rubber (CF-NR) composites have been studied at varying frequencies. The effects of alkali treatment, thermal treatment and a three-component dry bonding agent consisting of hexamethylenetetramine, resorcinol and nano silica (HRS) on these properties were studied. Dicumyl peroxide (DCP) and sulphur were used as curing systems in the preparation of the composites. Fibre filled composite systems have higher values of dielectric constant than the gum (unfilled) sample. This is due to the polarization exerted by the addition of fibres into the matrix. The dielectric constant decreases with frequency due to the dropping out of dipolar and interfacial polarization at higher frequency. The dielectric constant values of composites containing alkali treated chicken feather fibres (ACF) were higher because of the increase in number of polar groups after the treatment. The carbonized chicken feather fibre (CCF) incorporated NR composites have highest dielectric constant values because they consist of conducting material in an insulating matrix which leads to interfacial polarization. The dielectric constants of sulphur cured composite samples are higher than the corresponding DCP cured ones. The addition of fibres and with the incorporation of the bonding agents causes an increase in the dielectric constant and decreases the volume resistivity of the composites.

**Keywords:** Natural rubber, Chicken feather fibre, Dicumyl peroxide, Dielectric properties, Bonding agent

## Introduction

Polymers are generally good electrical insulators and are commonly used in the electronics industry for housings and assemblies. For antistatic applications and shielding against electromagnetic interference, electrical conductivity of rubber and plastic compounds is an important factor [1]. For specific applications, polymers are made conductive by adding metals, carbon black and conductive fibres. Electrical conductivity can be combined with desirable physical properties by incorporation of a conducting polymer into a host polymer substrate to develop a blend, composite or an interpenetrating network. The composition, chemical structure, physical texture as well as the conditions of measurement influence the process of conduction through a polymeric system [2].

Substantial information about the chemical and physical states of polymers can be obtained from dielectric properties such as the dielectric constant and the dielectric loss. These properties vary with the method of preparation, molecular structure and crystal structure. External factors such as frequency of the applied voltage and temperature also influence it [3]. Natural rubber (NR) has high value of permittivity and reasonably good insulating properties. Considerably high dielectric loss values of NR causes to lose its insulating properties. Haseena *et al*. [4] explained the dielectric properties and the conduction mechanism of sisal-coir hybrid fibre reinforced natural rubber composites. Honey John *et al.* [5] prepared different compositions of conducting NR with polyaniline (PANI) semi interpenetrating networks and determined their dielectric properties in microwave frequency. Jayamani *et al.* [6] analysed the dielectric properties of composites poly lactic acid with different lignocellulosic fibres. Pervoskite ($BaTiO_3$) nanoparticles were charged into NR matrix reinforced with conventional stabilizer additives by Gonzalez *et al.* [7]. The dielectric elastomer becomes more insulating with the addition of nanometric oxide ($BaTiO_3$) particles. Ward *et al.* [8] studied the effect of phosphate pigment on dielectric properties of NR and NR-Acrylonitrile budtadiene rubber (NBR) blend and compared it with the effect of carbon black. It was found that there is correlation between the variation of dielectric properties with phosphate pigment and mechanical properties of the composites. Matchawet *et al.* [9] studied the effect of carbon black on electrical conductivity and dielectric constant of the epoxidized NR-50 matrix. Curing characteristics and dielectric properties of NR-Graphite composite was compared with NR-Carbon Black composite by Ravikumar *et al.* [10] and it was found that the latter is more conductive than former.

Keratin fibre from waste chicken feather is quite attractive from an economic and environmental point of view for developing a dielectric material. CF has alpha helix structure at the molecular level and is light and tough to endure mechanical and thermal stress. The nodes and hooks present in the hollow structure helps to improve the structural properties and increase the surface area. Since the fibre has a hollow structure, a given volume of it naturally contains a

---

*Corresponding author: rajeshvlcy@rediffmail.com

substantial volume of air resulting in low density, 0.80 g/$cm^3$, and low dielectric constant. Air is ideal dielectric materials, with the lowest dielectric constant of 1.0, through which signals can travel faster. These fibrils have an aspect ratio > 1000 [11].

Mishra *et al.* [12] developed novel composite material with chicken feather fibrils as reinforcement in epoxy resin matrix and investigated the dielectric characteristics at different temperature and frequency. Such composites were found to have potential use as a low dielectric material for typical applications. The properties of composites with epoxy, chicken feather fibre (CFF), and E-glass fibres for potential applications as printed circuit boards (PCBs) was investigated by Zhan *et al.* [13]. It was found that the hybrid fibre composite has a good balance of properties and costs, while being more sustainable.

Kiew *et al.* [14] studied the electrical properties of composites of chicken feather fibre (CFF) and kenaf fibre (KF) with unsaturated polyester (UP) composites. The dielectric constant, dissipation factor, and loss factor of CFF-UP composite were lower compared to the kenaf fibre-UP composites. The results indicated the application potential of CFF composites in high speed printed circuit board (PCB) material with good frequency stability at 1 MHz. Composites of chicken feather fibre with unsaturated polyester matrix modified with maleic anhydride can also be used as a PCB material as revealed by the investigations of Hamdan *et al.* [15].

Recently in our laboratory, we developed a new composite with chicken feather fibre (CF) as filler in natural rubber matrix. We have studied the effect of fibre loading, alkali treatment of fibre, curing systems and the bonding agent (HRS system) on the cure characteristics and mechanical properties of CF reinforced NR composites [16]. The objective of the present work is to examine the dielectric properties of the composites consisting of natural rubber (NR) and chicken feather fibre (CF). The dielectric properties of the composites have been analyzed with special reference to effects of fibre loading, various fibre treatments and a bonding agent. Incorporation keratin fibres into NR matrix increases the affinity of CF-NR composites to water and shows a higher electric conduction due to the hydrophilic properties of the incorporated protein fibres and hence the keratin-elastomer composite obtained from CF and NR seems to be of significant importance in practical applications such as the production of conductive flexible seals, gaskets and conductive mats used to prevent electrostatic damage to electronic devices.

## Experimental

### Materials

Natural rubber (Product No.ISNR-5) used for the study was procured from Indian Rubber Research Institute at Kottayam, Kerala. The processing additives, such as dicumyl peroxide (DCP, 40 % active, CAS No.80-43-3), sulphur, zinc oxide (ZnO, CAS No.1314-13-2), stearic acid (CAS No.57-11-4), mercapto benzothiazoledisulphide (MBTS, CAS No.120-78-5) and tetramethyl thiurammonosulphide (TMT, CAS No.120-78-5) were obtained from Joefex Chemicals, Kottayam, India. The common chemicals such as sodium hydroxide (NaOH, CAS No.1310-73-2) resorcinol (CAS No.108-46-3) and hexamethylenetetramine (CAS No.100-97-0) were obtained from Merck India Ltd. The nanosilica (CAS No.7631-86-9) used in the study was supplied by Sigma Aldrich, India.

### Processing of Chicken Feather Fibre

Waste chicken feather was collected from a nearby poultry farm. It was washed and dried in sunlight. Barbs were manually cut from the rachis of feathers and used directly as filler in raw chicken feather fibre (RCF)-NR composites. RCF was dipped in 2 % aqueous solution of sodium hydroxide for two hours and then washed in running water followed by drying in a hot air oven at 60 °C for 6 hours to get alkali treated chicken fibre (ACF). Thermal modification of CF is carried out by semi carbonization at 220 °C in muffle furnace without atmospheric control for 24 hours and carbonization at 450 °C by pyrolysis for preparing carbonized chicken feather fibre (CCF) (Scheme 1).

### Composites Preparation

Composites were prepared by mixing NR with the additives in a two roll mill according to ASTM-D 3184 procedure [17]. Uniform dispersion of fibres was ensured by adding them in small increments. After thorough mixing, the composites were sheeted out through a tight nip to orient the fibres unidirectional. Table 1 and 2 show the formulations of composites. Gum sample denotes the mix without any fibre loading. The sheets were vulcanized at 150 °C in a hydraulic

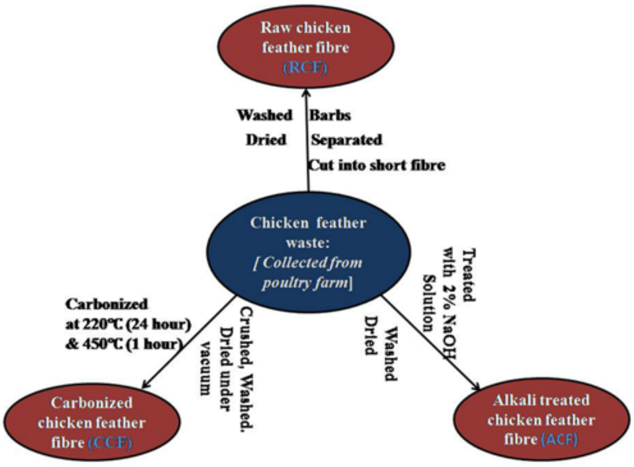

**Scheme 1.** Processing of chicken feather fibres.

**Table 1.** Formulation of CF-NR composites (phr*, DCP vulcanization)

| Sample code | NR[a] | DCP[b] | RCF[c] | ACF 2[d] | CCF[e] | Hexa[f] (H) | Resorcinol (R) | Nano silica (S) |
|---|---|---|---|---|---|---|---|---|
| GUM | 100 | 2.5 | .... | .... | | …. | …. | ..... |
| RCF-NR (5,15,25,30) | 100 | 2.5 | 5,15,25,30 | .... | | …. | …. | ..... |
| ACF 2(25)-NR | 100 | 2.5 | .... | 25 | | .... | .... | .... |
| CCF (25)-NR | 100 | 2.5 | .... | .... | 25 | .... | .... | .... |
| RCF(25)NR(HRS) | 100 | 2.5 | 25 | .... | | 4 | 6.3 | 2.5 |
| ACF(25)NR(HRS) | 100 | 2.5 | | 25 | | 4 | 6.3 | 2.5 |

*Parts per hundred rubber, (a) natural rubber, (b) dicumyl peroxide, (c) raw chicken feather fibre, (d) alkali treated chicken feather fibre in 2 % NaOH solution, (e) carbonized chicken feather fibre, and (f) hexamethylenetetramine.

**Table 2.** Formulation of CF-NR composites (phr*, Sulphur vulcanization)

| Compounding ingredients | Sample code | | | | | |
|---|---|---|---|---|---|---|
| | GUM | RCF(25)NR | RCF(25) NR-HRS | ACF 2(25)NR | ACF 2(25) NR-HRS | CCF(25)NR |
| NR | 100 | 100 | 100 | 100 | 100 | 100 |
| ZnO | 5 | 5 | 5 | 5 | 5 | 5 |
| Stearic acid | 2 | 2 | 2 | 2 | 2 | 2 |
| MBTS[a] | 1.5 | 1.5 | 1.5 | 1.5 | 1.5 | 1.5 |
| TMT[b] | 0.5 | 0.5 | 0.5 | 0.5 | 0.5 | 0.5 |
| Sulphur | 2.5 | 2.5 | 2.5 | 2.5 | 2.5 | 2.5 |
| RCF | --- | 25 | 25 | --- | --- | --- |
| ACF 2 | --- | --- | --- | 25 | 25 | --- |
| CCF | --- | --- | --- | --- | --- | 25 |
| Hexa | --- | --- | 4 | --- | 4 | --- |
| Resorcinol | --- | --- | 6.3 | --- | 6.3 | --- |
| NanoSilica | --- | --- | 2.5 | --- | 2.5 | --- |

[a]Mercaptobenzothiazyldisulphenamide and [b]tetramethylthiurammonosulphide.

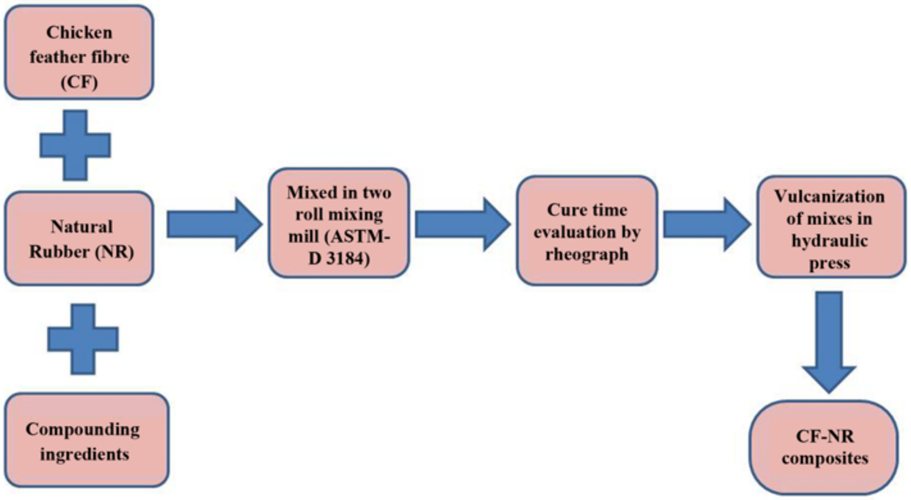

**Scheme 2.** Composite preparation procedure.

press to the optimum cure time obtained by using a rheometer (Goettfert elastograph, Germany) (Scheme 2).

### Evaluation of Dielectric Properties

Dielectric properties were measured using square shaped samples having a thickness of 0.5 mm and area of 160 mm$^2$. Conductive copper tapes with a thickness 0.05 mm fixed on both sides of the samples were used as electrodes. Impedance Analyzer (6500 B, Wayne Kerr, UK) was used to measure the capacitance, resistance and dissipation factor. The quantities were measured at varying frequencies ranging from 10 kHz to 10 MHz as per ASTM standard D-150 [18].

#### *Dielectric Constant*

For an insulating material dielectric constant is the ratio of the charge stored in the material placed between two metallic plates to the charge stored when the material is replaced by air (or vacuum). The dielectric constant, E was determined from capacitance using the equation:

$$E' = Ct/E_0A \tag{1}$$

where $C$ is the capacitance; $t$, the thickness; $E_0$, the permittivity of air ($8.85\times10^{-12}$ F/m); and $A$, the area of cross-section of the samples.

#### *Dissipation Factor*

Dissipation factor is the electrical loss or the amount of energy dissipated by the insulating material when the voltage is applied to the circuit. Elastomers generally have lower dissipation factor at room temperature. The loss factor (dielectric loss, E″), the dielectric constant (E′) and the dissipation factor (tan δ) are related by the equation:

$$\tan\delta = E''/E' \tag{2}$$

#### *Conductivity*

The effective conductivity due to the electric polarization is represented as:

$$\sigma = \omega E_0 E'' = \omega E_0 \tan\delta E' \tag{3}$$

where ω represents the angular frequency i.e. ω = 2πf, where f is the frequency.

#### *Volume Resistivity*

The volume resistivity (ρ), which measures the insulation resistance of a material, has been calculated by using the equation:

$$\rho = 1/\sigma \tag{4}$$

### Fourier Transforms Infrared (FTIR) Spectroscopic Analysis

FTIR spectra were recorded using FTIR spectrophotometer (IR Affinity 1S-Shimadzu, North America) in the range of 600-4000 cm$^{-1}$ with a resolution of 4 cm$^{-1}$ and 45 numbers of scans.

### Thermal Properties

The thermal stability study of CF-NR composites was carried out using Thermo gravimetric analyzer (TGA 50, Shimadzu, North America). The heat flow and glass transition temperature ($T_g$) of composite systems were measured by using a DSC 7 calorimeter (Perkin Elmer, UK).

### Scanning Electron Microscopic (SEM) Studies

The surface morphology of the fracture surfaces of composites were examined using scanning electron microscope (model: FESCA, SU6600 FESEM, Hitachi, Germany).

## Results and Discussion

### Dielectric Constant

The term dielectric constant (E′) of a polymer is a measure of its ability to store charges. It depends on the polymers, type of filler and loading level. Dielectric constant of a composite material generally arises due to the polarization of the molecules. Usually the dielectric constant shows an increase with polarizability of material. Interfacial, orientation, atomic and electronic polarizations contributes to the dielectric constant of a composite. The interfacial polarization takes place in composite due to the differences in the polarizations of the matrix and fillers. When polymers containing polar groups are placed in an electric field, orientation polarization occurs. Concentration of fillers significantly affects both the orientation and interfacial polarization of a composite [4,19].

Figure 1 shows the effect of fibre loading on the dielectric constant (E′) values of chicken feather fibre reinforced NR composites as a function of logarithm of frequency. As the fibre loading increases the dielectric constant increases at all frequencies. Lowest E′ value is exhibited by the gum sample due to the absence of permanent dipoles. In general, the frequency dependence of E′ is controlled by the polarity of

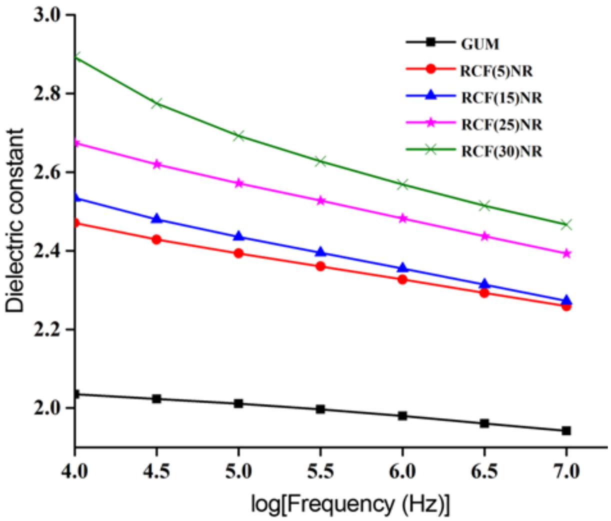

**Figure 1.** Effect of RCF loading on dielectric constant of CF-NR composites as a function of frequency.

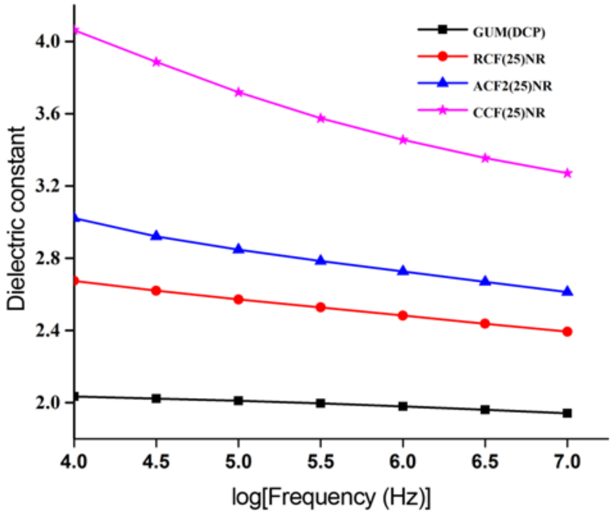

**Figure 2.** Effect of various treatments of CF on dielectric constant of CF-NR composites as a function of frequency at 25 phr loading.

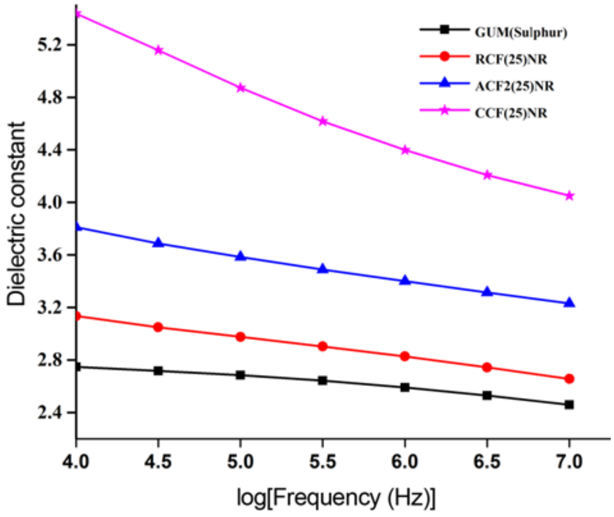

**Figure 3.** Effect of sulphur curing systems on dielectric constant of CF-NR composites as a function of frequency at 25 phr loading.

the polymer. The increase in dielectric constant with fibre loading is due to the presence of polar groups of keratin in RCF which causes an increase in orientation and interfacial polarization. For a given fibre loading, the values of E′ are higher at lower frequencies. This is due to the fact that complete orientation of the molecules is possible only at lower frequencies and that orientation polarization requires more time to reach the equilibrium static field value compared to electronic and atomic polarizations. Therefore as frequency increases the E′ reduces due to the lag in orientation polarization [4,20].

Figure 2 shows the effect of alkali and thermal treatments of CF on the dielectric constant values of CF-NR composites at 25 phr loading. At all frequencies dielectric constant values of treated fibrous composites are higher than the untreated one. This is because of the increase in orientation polarization as a consequence of the improved hydrophilicity of the alkali treated fibres. The alkali treatment of fibres destroys the hydrogen bonding of hydroxyl groups (-OH) of the fibres and thereby makes them more reactive. The wax and the lipid component of RCF undergo dissolution and leaching by alkali treatment which cause an increased interlocking between ACF and NR matrix, resulting in stronger composites [16]. The probability for the interaction between polar -OH groups of fibres and water molecules also increases the moisture absorption tendency of the fibres and thus ACF composites show a substantial increase in dielectric constant values compared to the RCF composites. The higher value of dielectric constant of CCF-NR composite in lower frequency range compared to the fibrous CF composites can be due to the interfacial polarization (IP) or Maxwell-Wagner (M-W) polarization, which occurs due the presence of electrically heterogeneous materials [10]. The interfacial polarization in such systems, is caused by the dispersion of conductive filler in the insulating polymer matrix. The permanent dipoles formed by CCF at the polymer-filler interfaces enhance the ability for polarization and improve the dielectric constant. These dipoles are comparatively bigger in size than orientation, ionic and electronic dipoles. When the frequency increases, the induced dipoles do not get sufficient time to align in the direction of applied electric field and hence dielectric constant is reduced. The dielectric constant of CF-NR composites decreases in the order, CCF > ACF > RCF.

Figure 3 shows the dielectric constants of sulphur cured CF/NR composites containing 25 phr CF. By comparing Figure 2 and Figure 3, it can be seen that DCP cured sample has lower value of dielectric constant than the corresponding sulphur cured one at all frequencies. The difference in behavior is due to the cross-linking reaction of NR with peroxide. The free-radical reaction between NR matrix and CF fibres initiated by peroxide is as follows [4,21]:

$$\text{R-O-O-R} \longrightarrow 2\text{RO}^{\bullet}$$

$$\text{RO}^{\bullet} + \text{NR-H} \longrightarrow \text{ROH} + \text{NR}^{\bullet}$$

$$\text{RO}^{\bullet} + \text{Fibre-H} \longrightarrow \text{Fibre}^{\bullet} + \text{ROH}$$

The hydrogen may be abstracted from the -OH or -CH bonds of the keratin, as well as from the carboxyl (-COOH) group. Grafting of NR and fibres takes place by combining two radicals.

$$\text{NR}^{\bullet} + \text{Fibre}^{\bullet} \longrightarrow \text{NR-Fibre}$$

These results in the reduction of hydrophilicity of fibre and hence lower value of dielectric constant for DCP cured composite.

Figure 4(a) and (b) shows the effect of different curing system and bonding agents on the dielectric constants of the

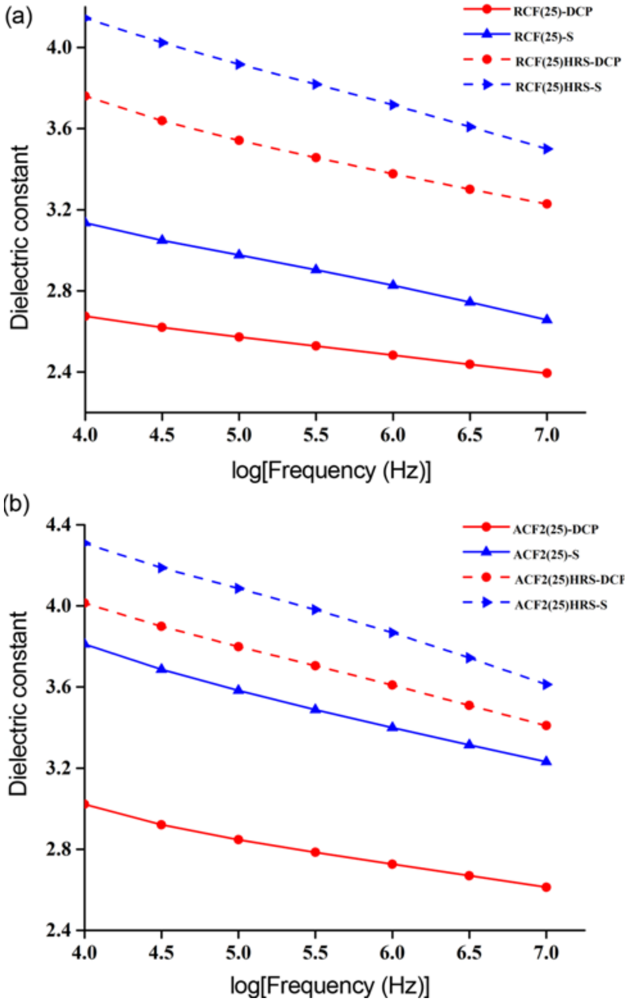

**Figure 4.** Effect of different curing system and HRS bonding agents on the dielectric constants of (a) RCF and (b) ACF composites as a function of frequency at 25 phr loading.

RCF and ACF composites. The dielectric constant of bonding agent added composite shows a high value. It can also be seen that sulphur cured sample has higher dielectric constant than DCP cured one in the presence of bonding agent also. A three-component bonding system consisting of hexa, resorcinol and nano silica was used for the present composite system. An in-situ resin formation takes place by the condensation reaction between resorcinol, hexa and nano silica as the vulcanization proceeds. The hexa donates methylene (-$CH_2$) groups to resorcinol to form a resin, which helps in binding the CF fibres and NR matrix together. The -OH groups in resorcinol is attributed to permanent dipoles and the difference in total polarizability of the bonded systems. Thus the dielectric constant is increased due to the modification of interface [4,22].

### Volume Resistivity

The most desirable property of an insulator is its ability to

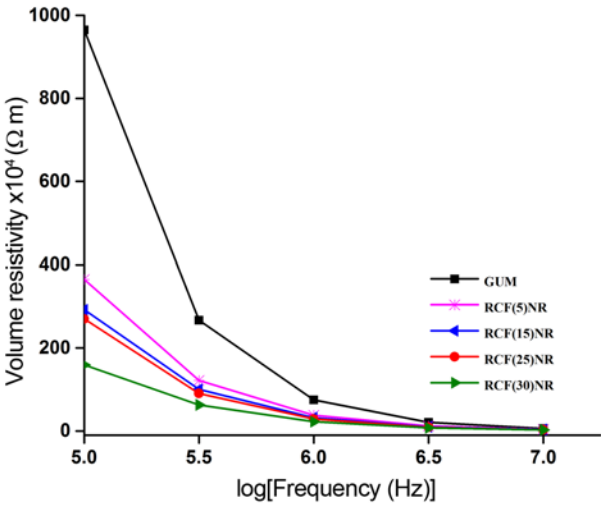

**Figure 5.** Effect of RCF loading on the volume resistivity of CF-NR composites as a function of frequency.

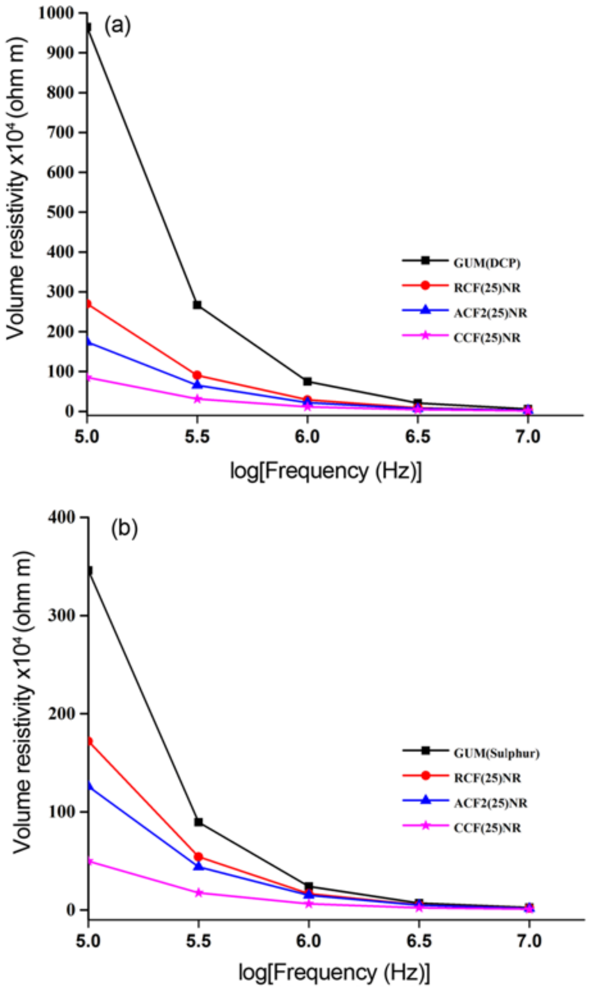

**Figure 6.** Effect of different curing system on the volume resistivity of RCF, ACF and CCF composites as a function of frequency at 25 phr loading.

resist the leakage of electric current which is measured as the volume resistivity. The variation of volume resistivity with fibre loading at different frequencies is represented in Figure 5. The volume resistivity decreases with increase in frequency and fibre loadings. When the CF fibres are added to NR, polarization process is facilitated due to the presence of polar groups in fibre and hence the resistivity decreases.

Figure 6 shows the effect of different curing system on the volume resistivity of RCF, ACF and CCF composites. Treated composite has lower volume resistivity than that of the untreated one. In any polymeric materials current mostly flows through the crystalline regions where as the flow of current through amorphous region occurs mainly due to the presence of moisture [23]. The alkali treatment of fibre surface increases the moisture absorption capacity, which leads to an increase in polarization and hence decreases in volume resistivity of the composites containing ACF compared to RCF. It is found that, the addition of CCF into NR matrix also decreases the resistivity of composites. This may be due to the higher conducting nature of carbonized CF. The resistivity decreases with increasing frequency (f) because of the increase in conductivity (σ), which is given by the equation (5).

$$\sigma(f) \sim f^{s} \text{ ($s$ arbitrary constant} \sim 0 \text{ to } 1) \tag{5}$$

The dependence of ac conductivity on frequency can be described by the Maxwell-Wagner (M-W) two layer models or the heterogeneous model [10]. From the analysis of resistivity of NR/RCF, NR/ACF and NR/CCF composites, it is found that CCF is better than ACF and RCF as conducting filler. It can also be seen that the resistivity of DCP cured sample is higher than sulphur cured one due to the different cross links present in two systems.

The variation of volume resistivity, as a function of frequency, for bonding agent added composites is given in Figure 7. The dielectric constant is related to resistivity by the equation [3]:

$$\log R \text{ (298K)} = 23 - 2E' \text{ (298 K)} \tag{6}$$

It is evident from the equation that as the dielectric constant increases the electrical resistance of composites decreases exponentially. It can be seen from Figure 7, the composite containing bonding agents has lower value of volume resistivity than that of the corresponding one without bonding agent which is attributed to the increase in polarizability. Bonded composite cured by DCP has higher volume resistivity than that cured by sulphur. The difference in behaviour is due to the difference in the total polarizability.

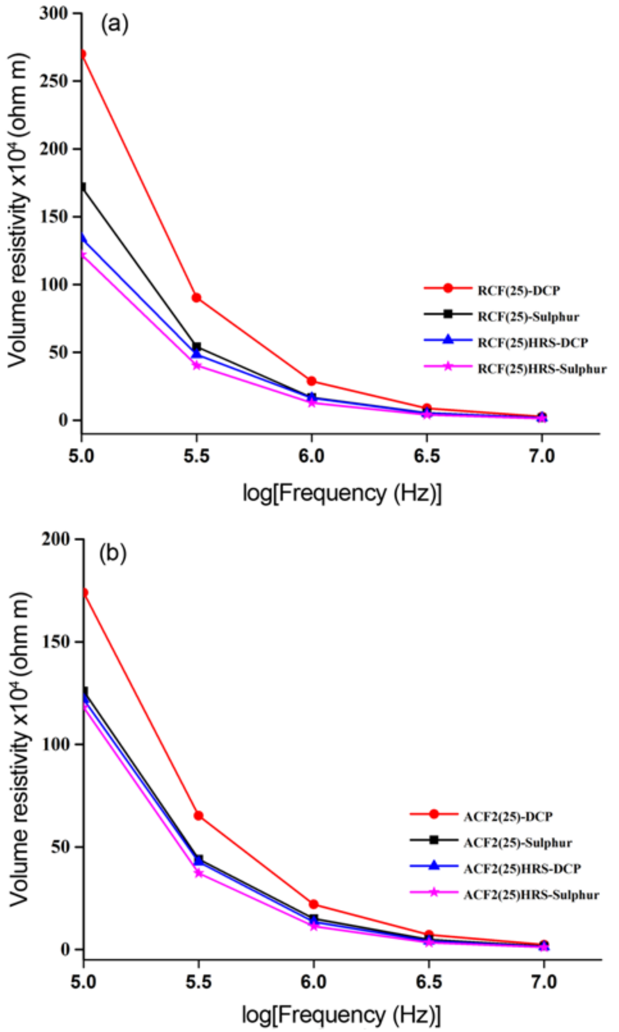

**Figure 7.** Effect of different curing system and HRS bonding agents on the volume resistivity of (a) RCF and (b) ACF composites as a function of frequency at 25 phr loading.

## Conductivity

Figure 8 shows the variation of electrical conductivity (σ),

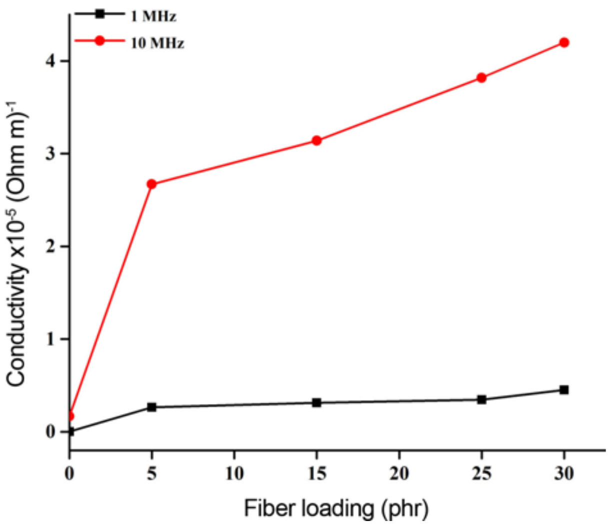

**Figure 8.** Effect of RCF loading on conductivity of RCF-NR composites.

with fibre loading at different frequencies (1 and 10 MHz). It can be seen that, as fibre concentration and frequency increase the conductivity increases. The increase in conductivity with fibre concentration is due to the increase in number of polar groups. As loading of fibre increases, the aggregates are more tightly packed and pressed against each other, resulting in the reduction of internal contact resistance. In an insulating material like fibre reinforced composites, pathways of lower resistivity must be extended throughout the sample for conduction to take place. This is what happens with increase in fibre concentration where the number of conducting phases increases and conductivity rises. Fibres those which are in agglomerates do not contribute to conductance.

## Dissipation Factor

For a capacitor, dissipation factor is the ratio of energy stored to that dissipated per cycle. It is a measure of energy lost during the reversal of electric polarization. It is used for evaluating the nature and quality of electrical insulation materials and systems. It measures the inefficiency of insulating materials. The dissipation factor (tan δ) of an insulating material is important as it measures the alternating current electrical energy which is converted to heat in an insulator. This heat rises the temperature of the insulator and accelerates its deterioration.

The effect of different fibre loading on dissipation factor (tan δ) as a function of the logarithm of frequency is given in Figure 9. The dissipation factor increases with fibre concentration and decreases with frequency. The curves of dissipation factor of filled systems are not identical with unfilled systems (gum). The curves of composites decrease steeply with frequency at first and then exhibit a gradual decrease. The value of tan δ of composites at specific frequency depends on the nature of relaxation and the relaxation which in turn is controlled by the polarity and carrier mobility [4]. The relaxation in the case of NR is due to the lag in electronic and atomic polarization. The amorphous phase relaxation is responsible for the increase in dissipation factor with frequency of NR. When the fibres are added, there is dipole relaxation of the polar groups and hence the dissipation factor increases. The dipole and charge carriers freely move within the material under test at lower frequency whereas they become unable to follow variation of the applied field at high frequency resulting in a decrease in dissipation factor.

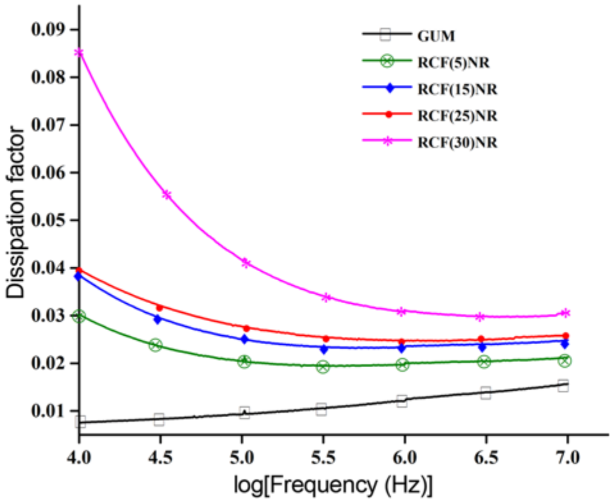

**Figure 9.** Effect of RCF loading on dissipation factor of CF-NR composites as a function of frequency.

Figure 10(a) shows the effect of various treatments on the dissipation factor of CF composites. The nature of treatment influences the magnitude of relaxation and the dissipation factor. Alkali treatment increases the relaxation magnitude at each frequency. The value of dissipation factor of CCF-NR is higher than that of RCF and ACF composites at the same loading of fibre. In CCF composites some space charges are generated at heterogeneous interface due to the difference in

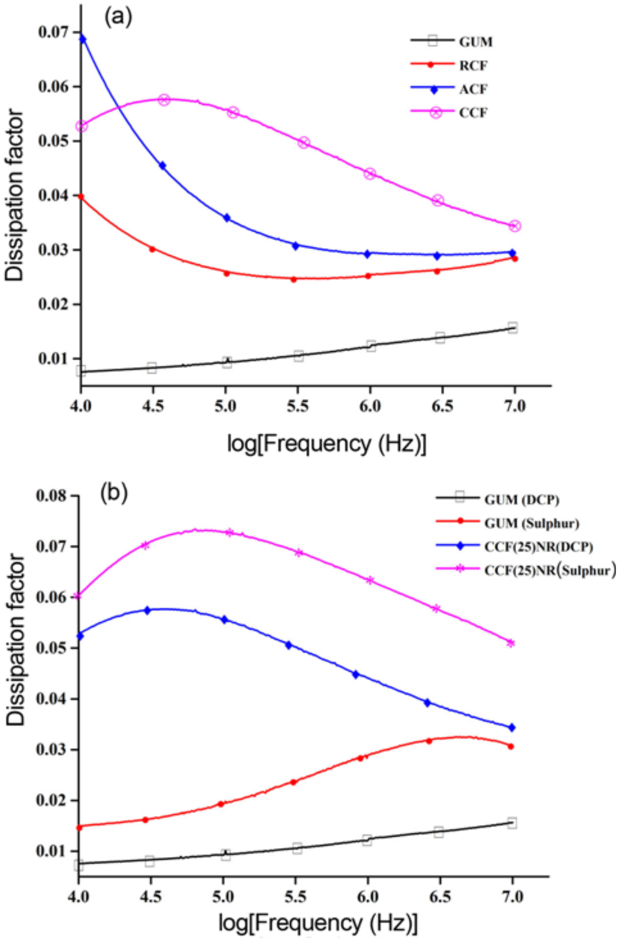

**Figure 10.** (a) Effect of various treatments of CF on dissipation factor of CF-NR composites and (b) effect of curing systems on dissipation factor of CCF composite as a function of frequency at 25 phr loading.

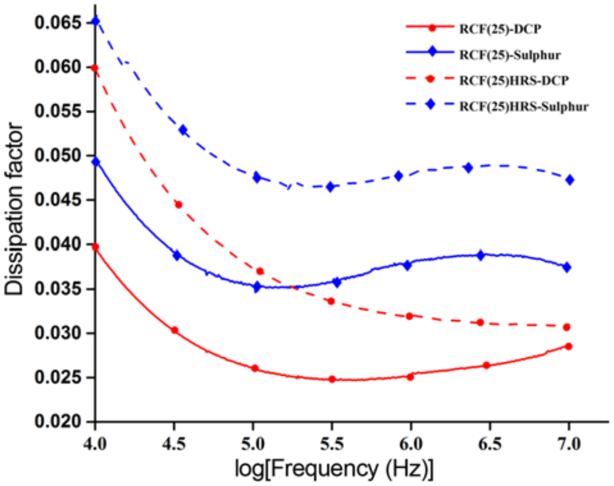

**Figure 11.** Effect of different curing system and HRS bonding agents on the dissipation factor of RCF composites as a function of frequency at 25 phr loading.

**Table 3.** FTIR peaks of functional group present in CF-NR composites

| Functional group present | IR peaks |
|---|---|
| O-H/N-H in the native secondary structure of protein in CF | 3300-3250 $cm^{-1}$ |
| Amide group NH symmetric stretch (Amide A) | 3273 $cm^{-1}$ |
| Amide group NH asymmetric stretch (Amide B) | 3075 $cm^{-1}$ |
| C-H stretching in the -CH=$CH_2$ group | 3033 $cm^{-1}$ |
| Symmetric and asymmetric stretching of aliphatic C-H group | 2960-2850 $cm^{-1}$ |
| valence vibration of homogeneous double bonds (C=C) in the NR structure | 1664 $cm^{-1}$ |
| Elongation of C=O of amide group (Amide I) | 1643 $cm^{-1}$ |
| Angular deformation in the N-H group and the stretching of C-N (Amide II) | 1535 $cm^{-1}$ |
| Angular deformation of $CH_2$ and $CH_3$ group | 1450 $cm^{-1}$ |
| deformation in plane of N-H and C=O group (Amide III) | 1270-1220 $cm^{-1}$ |
| Si-O-Si asymmetric stretching vibration in HRS bonded composites | 1082 $cm^{-1}$ |
| Si-O-Si symmetric stretching vibrations in HRS bonded composites | 785 $cm^{-1}$ |
| Akylthiol group (C-S stretching) from amino acid cystein | 730-620 $cm^{-1}$ |

conductivities of filler and matrix which lead to field distortion. This causes interfacial polarization which contributes to highest dissipation factor. The relaxation frequency of interfacial polarization is low and it decreases with increase of frequency and as a result dissipation factor also decreases with increase of frequency.

Figure 10(b) shows the effect of different vulcanizing systems on the dissipation factor of CCF composites. It can also be seen from the figure that the sulphur cured sample has higher value of dissipation factor than that of DCP cured one. Due to the flexible cross links introduced in presence of sulphur curing system, the charge carriers within the material can freely move and follow varying electromagnetic field and hence higher dissipation factor values compared to DCP cured samples.

Figure 11 shows the effect of HRS bonding agent on the dissipation factor of RCF composites. The dissipation factor of bonding agent added composites are higher than that of the unbonded one in both DCP sand sulphur vulcanizing systems. The curves of tan δ of DCP cured systems are not identical with sulphur cured systems due to the difference in relaxation mechanism.

## FTIR Spectroscopic Analysis

The fibrous structural protein found in CF is keratin; it is made up of amino acids that form a repeating secondary structure. Several functional groups present in keratin protein, especially in peptide backbone are disulfide (-S-S), amino (-$NH_2$), carboxylic acid (-COOH) and hydroxyl (-OH). The increase in dielectric constant with CF loading in NR is due to the presence of these polar groups of keratin in CF which causes an increase in orientation and interfacial polarization. The alkali treatment of CF destroys the hydrogen bonding of polar hydroxyl groups (-OH) of the fibres and thereby these -OH groups of fibres interact water molecules and also increases the moisture absorption tendency of the fibres and thus ACF composites show a substantial increase in dielectric constant values compared to the RCF composites. The peak associated with polar functional groups is clear from the FTIR spectra of RCF and ACF-NR composites (Table 4). The spectra of CF-NR composites and gum sample are very nearly identical and serve to confirm the belief that the curing causes changes in few of the polymer units which does not alter the rubber spectrum to any appreciable extent in composites. FTIR spectra of different CFs show that they are nearly identical. The only difference is in their rate of absorption. The intensity of peaks is increased in the spectra of ACF composites (Figure 12a and 12b) due to increase in absorption of these functional groups

**Table 4.** TG data of CF-NR composites at 25 phr loading

| Sample | DCP cured data | | | |
|---|---|---|---|---|
| | $T_{onset}$ (°C) | $T_{50\%}$ (°C) | $T_{max}$ (°C) | Residue % at 600 °C |
| GUM | 343.42 | 388.10 | 477.72 | 0.39 |
| RCF(25)NR | 347.92 | 387.01 | 573.94 | 0.43 |
| ACF2(25)NR | 352.89 | 389.50 | 614.83 | 3.38 |
| CCF(25)NR | 337.51 | 356.53 | 602.71 | 1.46 |

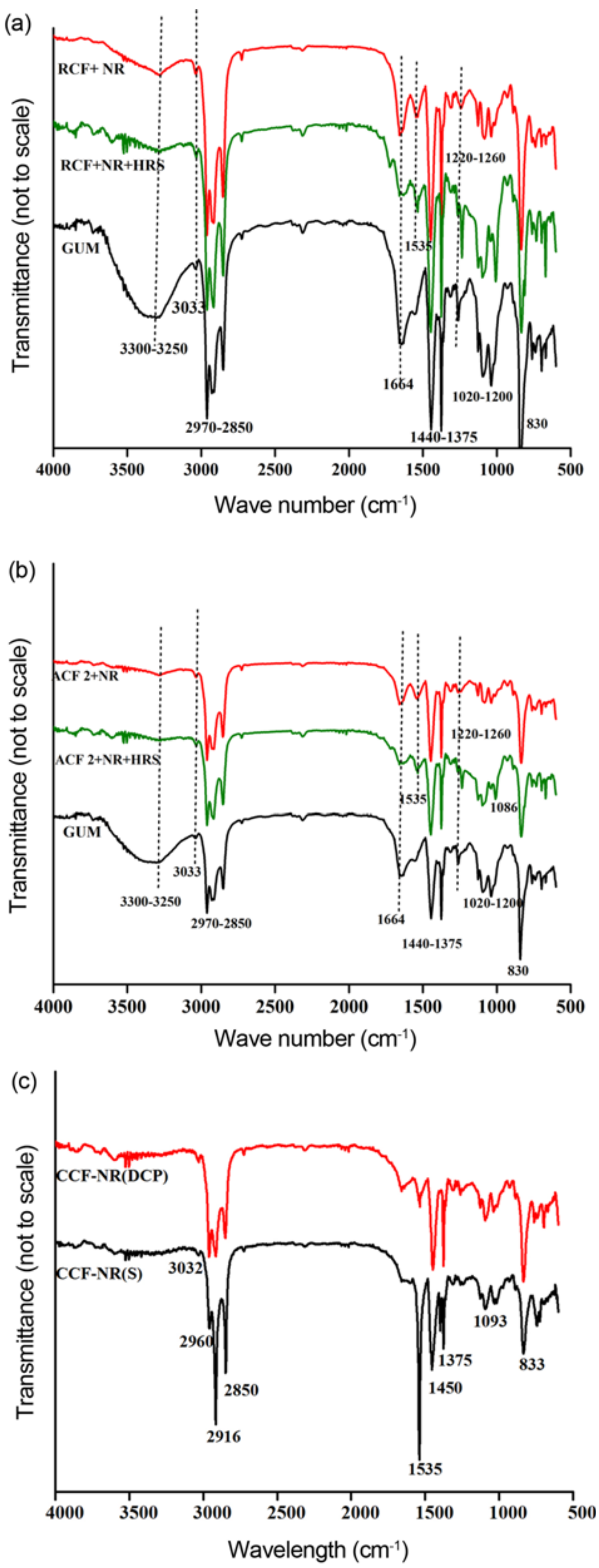

**Figure 12.** FTIR spectra of (a) RCF-NR composites at 25 phr loading, (b) ACF-NR composites at 25 phr loading, and (c) CCF-NR composites at 25 phr loading.

[16,24,25]. The absorption band located at 1086 cm$^{-1}$ is assigned to the Si-O-Si asymmetric stretching vibration in HRS bonded composites; the symmetric stretching vibrations of Si-O-Si appear at 785 cm$^{-1}$. Figure 12(c) shows the FTIR spectrum of CCF-NR composites with DCP and sulphur curing systems. It was noticed that the peak at 3075 cm$^{-1}$, is not visible in the spectrum, which means that the CF when carbonized, decrease the intensity of vibrations of amide B (associated with the stretching of the amide N-H) in this region. Peak at 1643 cm$^{-1}$ corresponding to amide I group extends a little for the CCF-NR spectra. Peak at 1535 cm$^{-1}$ which is characteristic amide II peak in CF perceived in the spectra with lesser intensity. In the CCF spectrum, there is no peak in the region between 1270 and 1220 cm$^{-1}$, suggesting that the N-H bond was broken and the C-N link in the backbone was fragmented [26].

## Thermo Gravimetric Analysis (TGA)

Figure 13a and b shows the TG and DTG curves of CF filled NR composite systems cured by DCP at 25 phr

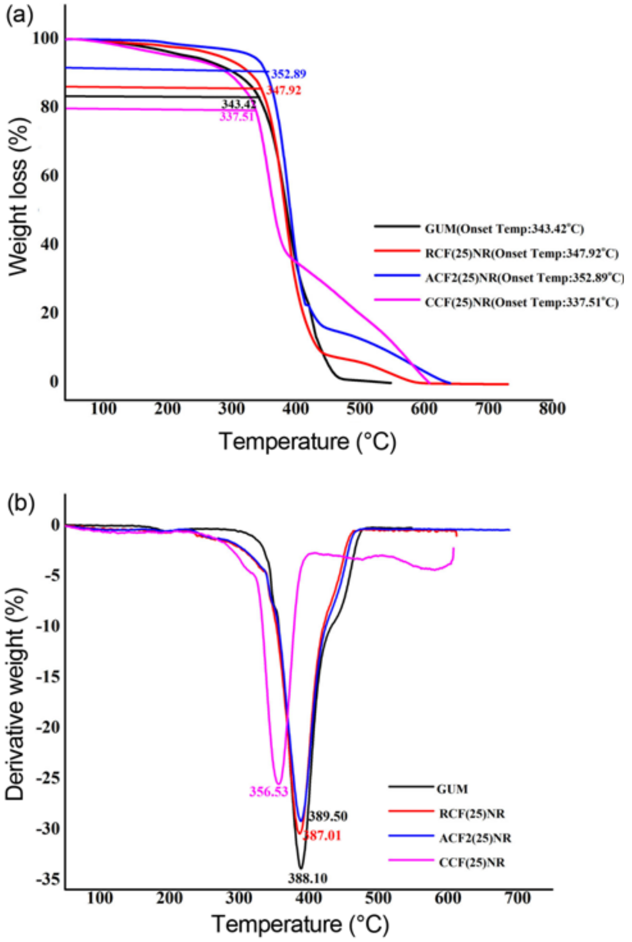

**Figure 13.** (a) TG and (b) DTG curves of CF-NR composites cured by DCP at 25 phr loading.

loading. Composite materials can be used up to high temperatures without degradation due to their good thermal properties such as thermal stability. The thermal stability of the composite can be determined with the onset temperature ($T_{onset}$), the temperature at which the decomposition begins. $T_{onset}$ is determined as the intersection point of the extrapolated baseline and the inflectional tangent of the temperature dependent heat flow signal at the beginning of melting crystallization point [27]. From the TGA curve of CF filled NR composites, it is clear that $T_{onset}$ of the gum sample is 343.42 °C. Taking the $T_{onset}$ of different CF-NR composites into consideration from the Table 4, it is noticed that thermal stability of NR matrix increases with effect of RCF and ACF in the matrix while the stability decreases under the influence of CCF. Alkali treatment of CF causes remarkable increment in the $T_{onset}$ and maximum degradation temperature of NR composites. Figure 13b shows derivative mass-temperature graphs of the CF-NR samples and it points out the temperature at which the highest decomposition rate of the gum and CF-NR biocomposite samples with 25 phr CF content. The decomposition temperature is indicative of materials resistance to temperature. In gum sample the highest degradation peak is at 388.10 °C. The thermal degradation behaviour of different CF-NR composites is found to be different and the lowest decomposition peak belongs to CCF-NR composite with 356.53 °C [27,28]. TGA results reveals that the thermal stability of NR composites is enhanced by CF reinforcement which act as a barrier for better heat insulation.

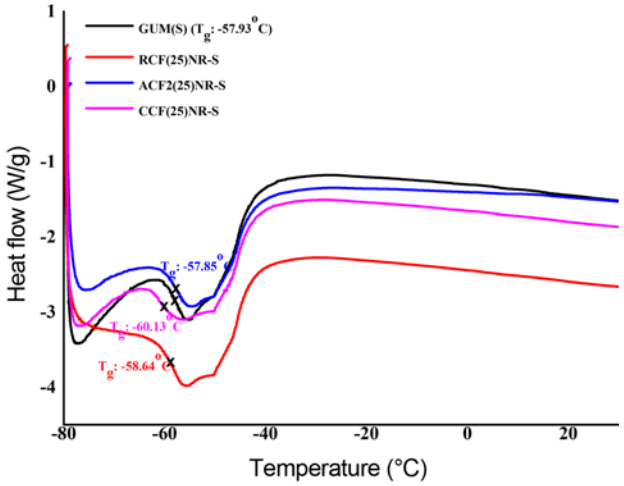

**Figure 14.** DSC curves of sulphur cured CF-NR composites at 25 phr loading.

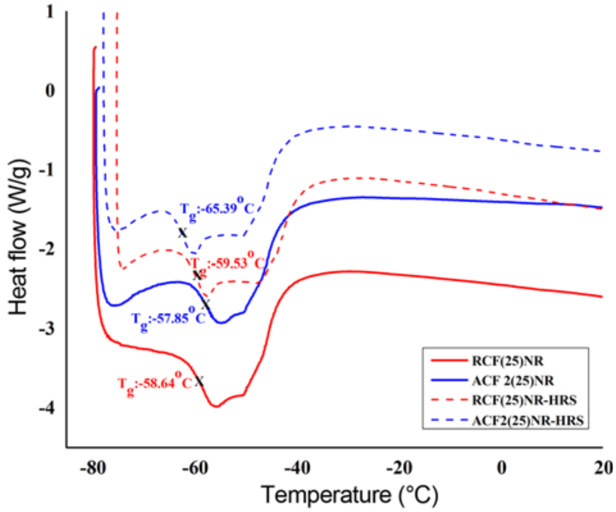

**Figure 15.** DSC curves of CF-NR composites with and without bonding agent at 25 phr loading.

## Differential Scanning Calorimetric (DSC) Studies

The DSC curves at heating rate 10 °C/min of CF-NR composites at optimum loading cured by sulphur are shown in Figure 14. DSC measures the flow of heat during an endothermic or exothermic process that develops in a controlled environment due to time and temperature function. In the DSC plot, the upper transition peaks indicate the heat requiring endothermic zone, while the down transition peaks reveal heat-releasing exothermic zone. The DSC curves of gum and composite samples show similar behavior which reveal that the crystallization behaviour is similar for NR and CF-NR composites. In the temperature range of -80 to -75 °C, a broad endotherm was observed due to dehydration. The second and strong endothermic peak corresponds to the glass transition found in the temperature range -60 to -50 °C. The glass transition is one of the most important properties of polymeric materials which refers to the temperature region ($T_g$) where the polymer changes from a rigid, glassy structure to a soft, rubbery structure. It is important to note that the glass transition do not occur suddenly at one unit temperature, but rather over a range of temperature. Hence an ideal way to determine $T_g$ is to draw a tangent on the initial straight line before the baseline shift and and another tangent on the slope and the cross over point is taken as $T_g$ (ASTM E1356-08) [27,29]. The $T_g$ of gum sample is -57.93 °C, the Tg of RCF-NR is -58.64 °C, the $T_g$ of ACF-NR is -57.85 °C whereas the CCF filled composite showed Tg at -60.13 °C. Composite samples have lower $T_g$ values than gum sample. $T_g$ of ACF sample is greater than the RCF and CCF samples. The lack of a trend in $T_g$ values may result not only from the non-homogeneity of the samples but also from the heterogeneity of the different parts of the samples. Figure 15 shows the DSC curves of hexa-resorcinol-nano silica (HRS) bonded RCF and ACF composite samples. It is observed that the $T_g$ value corresponding to the NR matrix slightly shifted to lower temperature range by the addition of the bonding agent in both RCF and ACF composites. More flexibility of non-crystalline NR matrix main chain may be

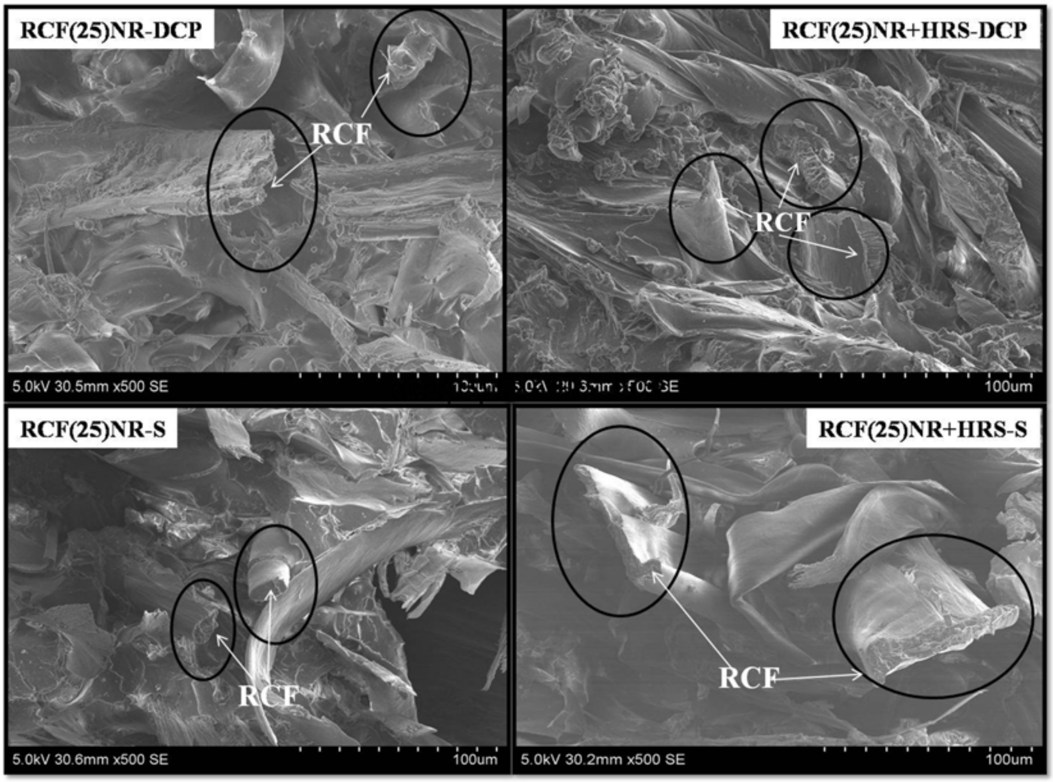

**Figure 16.** SEM micrographs of the tensile fractured surfaces of RCF-NR composites with and without bonding agent.

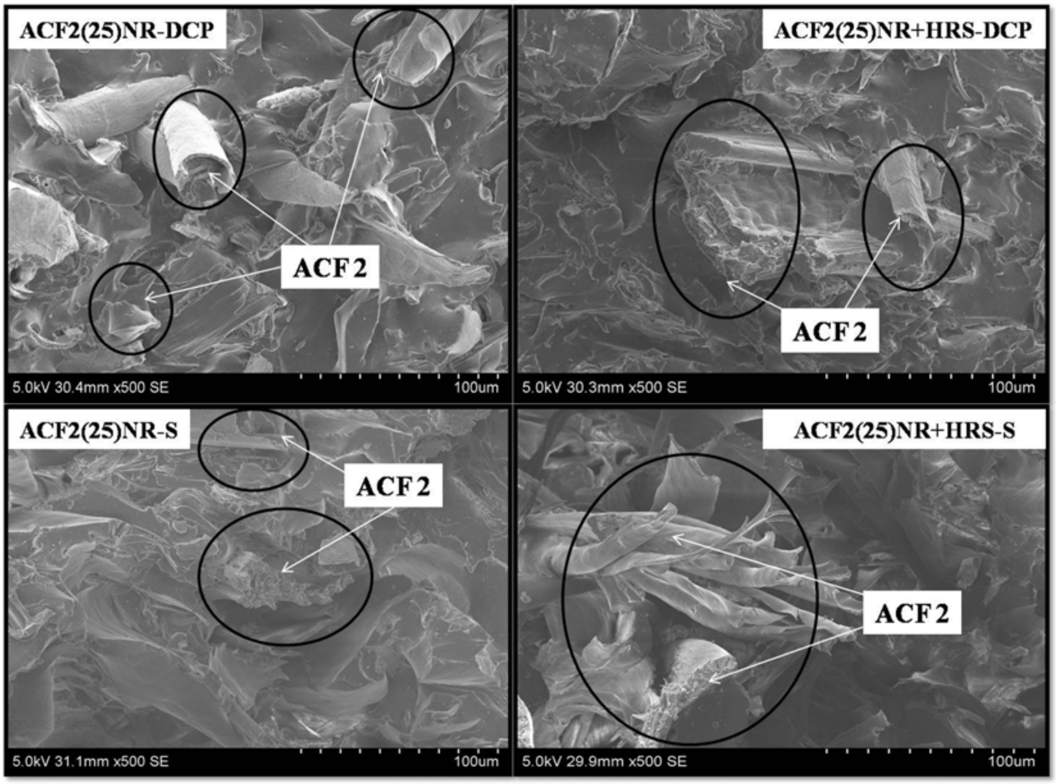

**Figure 17.** SEM micrographs of the tensile fractured surfaces of ACF2-NR composites with and without bonding agent.

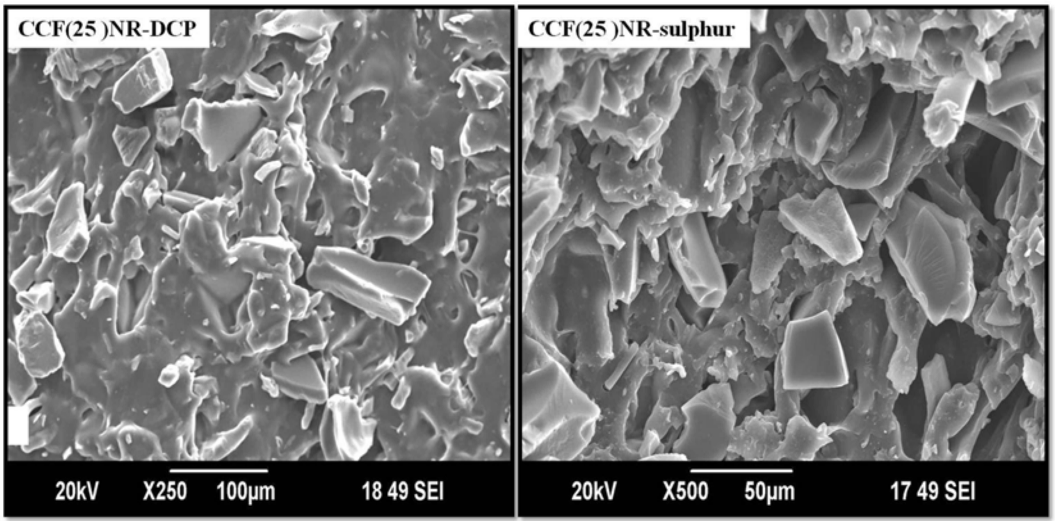

**Figure 18.** SEM micrographs of the tensile fractured surfaces of CCF-NR composites.

the reason for the lower $T_g$ values. According to DSC analysis, lowering of $T_g$ values of NR composites are noticed which associated with the easy processibility of CF-NR composites.

### Morphological Studies by SEM Analysis

The increased extent of adhesion between fibres and the matrix in bonding agent added composite systems has been further understood from the SEM micrographs of the composites. The SEM micrographs of the tensile fractured surfaces of composites containing 25 phr of RCF and ACF 2 with and without bonding agents using two different cross linking systems are shown in Figure 16 and Figure 17 respectively. The fibre ends can be seen protruding from the matrix. This confirms the longitudinal orientation, where the fibres are oriented perpendicular to the fracture front. Hence breakage of fibres takes place. In case of RCF composites, because of the weak interfacial adhesion between the fibre and rubber, fibre pullout may have taken place than breakage of fibres which left holes on the surface when stress was applied. Micrograph of ACF 2 composites shows the presence of broken fibres on the fracture surface, which was due to the strong adhesion between the fibre and rubber matrix for composites with alkali treated fibres. SEM studies also revealed that for composites without bonding agent, failure occurred at the weak fibre-rubber interface, whereas for composites containing treated fibre and bonding agent, failure occurred at the fibre due to strong adhesion between the fibres and matrix. Here the fibres well wetted by the rubber matrix [16,30]. SEM micrograph of CCF-NR composite in 25 phr loading is shown in Figure 18. The surface of CCF-NR composite showed the homogeneous CCF dispersion in NR matrix and also less agglomeration of CCF. The structure and dispersion of CCF affected the improvement in electrical properties of NR composites.

## Conclusion

The dielectric properties of chicken feather fibre reinforced (CF) natural rubber (NR) composites have been studied. The dielectric constant shows higher value at lower frequency region due to the interfacial polarization. As the fibre concentration increases, the dielectric constant of composites increases which is attributed to the increased orientation and interfacial polarizations.ACF and CCF composites show higher values of dielectric constant than the RCF composites for all frequencies. The dielectric constant of composite containing bonding agent show higher value. As the fibre loading increases the volume resistivity of the composite decreases. The conductivity of composites increases with increase in fibre loading due to the increase in number of conductive particles. Among all the CF-NR composites prepared CCF-NR composite exhibit the best dielectric properties. The value of dissipation factor of composites increases with increase in fibre loading. Composites with ACF and CCF have higher value of dissipation factor than those with RCF. The presence of HRS bonding agent improved the conductivity and dielectric constant of the CF-NR composite systems. TGA results confirmed the heat resistance exerted by the CF reinforcement in NR composites. Lowering of Tg values of CF incorporated NR composites shows the improvement in handling character of CF-NR composites. FTIR spectrum and SEM images of CF/NR composites give an additional support to the observations. The present low cost composite can be successfully used as good capacitors. CF-NR composites show a higher electric conduction due to the hydrophilic properties of the keratin fibres. The keratin-elastomeric composite obtained from CF and NR seems to be of significant importance in practical applications such as the production of conductive flexible seals and gaskets, and conductive mats used to prevent electrostatic damage to electronic devices.

## Acknowledgements

This work was financially supported by Kerala State Council for Science, Technology and Environment (KSCSTE), Thiruvananthapuram, Kerala, India. [Grant No. 228/2015/KSCSTE dated 22-6-2015]. This work was also supported by the instrumentation facility acquired through FIST funding of Department of Science and Technology, Govt. of India. [SR/FST/College-191/2014]. The Dielectric studies were conducted in high voltage lab of Electrical engineering department, National Institute of Technology, Calicut, Kerala, India.

## References

1. J. L. Acosta, M. C. Ojeda, and C. del Rio, *Polym. Bull.*, **57**, 199 (2006).
2. M. J. Miah, F. Ahmed, and A. H. Hossain Khan, *Polym.-Plast. Technol. Eng.,* **44**, 1443 (2005).
3. C. Rajesh, K. C. Manoj, G. Unnikrishnan, and E. Purushothaman, *Adv. Polym. Technol.*, **32**, E90 (2013).
4. A. P. Haseena, G. Unnikrishnan, and G. Kalaprasad, *Compos. Interf.*, **14**, 763 (2007).
5. H. John, R. Joseph, and K. T. Mathew, *J. Appl. Polym. Sci.*, **103**, 2682 (2007).
6. E. Jayamani, S. Hamdan, M. R. Rahman, and M. K. B. Bakri, *Materials Today: Proceedings,* **2**, 2757 (2015).
7. N. Gonzalez, M. A. Custal, S. Lalaouna, J. R. Riba, and E. Armelin, *Eur. Polym. J.*, **75**, 210 (2016).
8. A. A. Ward, S. H. El-Sabbagh, M. Ahmed Abd, and El-Ghaffar, *KGK Rubber Point*, **6**, 29 (2013).
9. S. Matchawet, A. Kaesaman, and P. Bomlai, *J. Compos. Mater.*, **50**, 2191 (2016).
10. K. Ravikumar, K. Palanivelu, and K. Ravichandran, *Materials Today: Proceedings*, **16**, 1338 (2019).
11. K. B. Jagadeeshgouda, P. Ravinder Reddy, and K. Ishwaraprasad, *Int. J. Res. Eng. Technol.*, **3**, 362 (2014).
12. S. C. Mishra and N. B. Nayak, *J. Reinf. Plast. Compos.*, **29**, 3016 (2010).
13. M. Zhan, R. P. Wool, and J. Q. Xiao, *Compos. Part A-Appl. Sci. Manuf.,* **42**, 229 (2011).
14. K. S. Kiew, S. Hamdan, and M. R. Rahman, *Bioresources*, **8**, 1591 (2013).
15. K. S. Kiew, S. Hamdan, and M. R. Rahman, *World Appl. Sci. J.*, **25**, 899 (2014).
16. D. P. Sreenivasan, A. Sujith, and C. Rajesh, *Mater. Today Commun.*, **20**, 100555 (2019).
17. ASTM-D-3184-89, "Standard Test Methods for Rubber-Evaluation of NR (Natural Rubber)", 2001.
18. ASTM D150-18, "Standard Test Method for AC Loss Characteristics and Permitivity (Dielectric Constant) of Solid Electrical Insulating Material", 2018.
19. A. A. Mamun and A. K. Bledzki, *Biofibre Reinforcements in Composite Materials*, doi: 10.1533/9781782421276.4.454 (2015).
20. C. C. Ku and R. Liepins, *British Polym. J.,* **21**, 181 (1989).
21. J. George, R. Janardhan, R. Anand, S. S. Bhagwan, and S. Thomas, *Polymer*, **37**, 3057 (1989).
22. A. W. Blum, "Phenolic Resins in Rubber Compounds", Rubber World, 2011.
23. D. S. Pramila Devi, T. Jabin, and S. K. Narayanan Kutty, *Polym. Technol. Eng.,* **51**, 823 (2012).
24. D. P. Sreenivasan, A. Sujith, and C. Rajesh, *J. Polym. Environ.,* **26**, 2720 (2017).
25. M. Prochoń, A. Przepiórkowska, and M. Zaborski, *J. Appl. Polym. Sci.*, **106**, 3674 (2007).
26. D. D. Belarmino and R. Ladchumananandasivam, *Brit. J. Eng. Technol.*, **1**, 1 (2013).
27. T. Akderya, U. Özmen, and B. O. Baba, *J. Polym. Res.*, **27**, 162 (2020).
28. C. E. Corcione and M. Frigione, *Materials*, **5**, 2960 (2012).
29. A. Kiziltas, D. J. Gardner, Y. Han, and H. S. Yang, *J. Thermal Anal. Calorim.*, **103**, 163 (2011).
30. L. Mathew and R. Joseph, *J. Appl. Polym. Sci.*, **103**, 1640 (2007).